Analysis of the high-Z impurity transport in a Tokamak by the IMPGYRO code

M. Toma[1], K. Hoshino[2], K. Inai[3], M. Ishida[1], A. Hatayama[1] and K. Ohya[3]

[1] *Faculty of Science and Technology, Keio University, Yokohama 223-8522, Japan*
[2] *Naka Fusion Institute, Japan Atomic Energy Agency 311-0193, Japan*
[3] *Institute of Technology and Science, the University of Tokushima, Tokushima 770, Japan*

(Received: 1 September 2008 / Accepted: 4 February 2009)

Transport process of high-Z tungsten impurities in a model geometry has been analyzed by the IMPGYRO code. The code includes most of the important process for high-Z imputities: 1) gyro-motion in the realistic magnetic configuration in tokamaks, 2) Coulomb collision and 3) multi-step ionization and recombination processes. Also, 4) re-emission (self-sputtering and reflection) process on the material surface has been taken into account by the direct coupling of the IMPGYRO code to the EDDY code. In this study, the numerical mesh for the analysis have been extended to the low density and temperature region in front of the wall, the baffle and the dome structure to take into account more correctly the re-emission/re-deposition process of high-Z impurity on these surfaces. The numerical algorithm of the code has been checked by the comparison of global-confinement time for a typical divertor detachment condition between numerical result and simple analytical result, and reasonable agreement has been obtained.

Keywords: divertor, impurity transport, tungsten, detach plasma, Monte Carlo simulation, plasma-surface interaction, self-sputtering, reflection

1. Introduction

Recently, tungsten has been paid attention as a divertor material which is not subjected to chemical sputtering. The radiation-cooling problem of core plasma, however, might arise even if a small amount of such high-Z impurities enters the core plasma region. Therefore, it is very important to understand the transport process of tungsten impurities in the SOL/divertor plasma region and to evaluate the amount of impurities that enter the core plasma.

For this purpose, we are developing the IMPGYRO code[1-3]. The final goal of the code development is to give an useful tool for the accurate evaluation and a reliable prediction of the impurity amount penetrating into the core in the future fusion reactors. The code numerically follows trajectories of impurity test neutrals/ions in realistic tokamak geometries. Important elastic/inelastic collisions with background plasma are included by the Monte-Carlo method.

The most distinct feature of the IMPGYRO code is that it takes into account directly the Larmor motion of high-Z impurity ions, instead of the guiding center approximation used in most of the conventional codes for the global impurity transport in edge plasmas. In addition, an attempt to couple the IMPGYRO code with the EDDY (Erosion and Deposition based on DYnamic model) code [4] has been started. This coupling makes it possible to analyze not only the large-scale transport process of high-Z impurities in the edge plasmas, but also to analyze self-consistently the surface processes of solid (e.g., erosion by sputtering, re-emission and deposition process, etc.). Quite recently, the initial test calculations of the IMPGYRO-EDDY coupling have been done in Ref. [4]. In these test calculations, however, a relatively simple assumption has been made for the boundary condition. The surface re-emission process (self-sputtering and reflection) were assumed to take place only on the divertor plate. The remaining calculation boundaries, such as the first wall, baffle plate, dome structure in the divertor region, were assumed to be absorbing boundaries. Test impurity particles reaching these absorbing boundaries were simply removed from the system without reflection and/or the self-sputtering processes.

In the present study, we have improved the mesh generation technique to remove the above assumption. The test calculations have been done again with the coupled IMPGYRO-EDDY code under almost the same calculation conditions in Ref. [4] except for the above boundary condition. In Sec. 2, a brief summary of the model implemented in the IMPGYRO code is given. Numerical meshes used in the present study will be compared with those in the previous study[4], in relation to the boundary condition for test particles. The results of the coupled IMPGYRO and EDDY code for a typical detached plasma are given in Sec. 3 with more realistic boundary condition. The comparison will be made with the previous results using relatively simple boundary condition. Also, the dominant transport path of high-Z impurity toward the core and other surrounding walls (divertor plate, dome, baffle plate, and first wall) will be discussed in Sec. 3.

author's e-mail: toma@ppl.appi.keio.ac.jp

2. Simulation model and calculation conditions

2.1 Brief summary of the physics model implemented in the IMPGYRO code

The IMPGYRO code includes most of the important process/effect to analyze the transport processes on fusion edge plasma: 1) gyro-motion of test impurity particles in realistic tokamak geometry[2,3], 2) Coulomb collision with background hydrogen plasmas[5] and thermal force[6], 3) multi-step ionization and recombination processes[7], 4) impurity surface-interaction process (self-sputtering process, reflection process, etc.).

To improve the surface-interaction model, recently the IMPGYRO code has been coupled to the EDDY code[8]. The EDDY code simulates the slowing down of incident ions in the material and the formation of recoil cascades leading to processes such as ion reflection and physical sputtering. The coupling has been done in the following manner[4]. The IMPGYRO code follows test impurities in the plasma region. If a test particle hits the material surface, the incident energy and angle of the test particle are transferred to the EDDY code. From these input parameters, the EDDY code calculates the number of sputtered and/or reflected particles, their emitted energies and angles from the material surface. Then, each trajectory of sputtered/reflected particles in the plasma is again followed by the IMPGYRO code. This procedure is repeated until the impurity density reaches the steady state. More detailed explanation of each models are given in references cited above.

2.2 Background plasma condition

The background plasma profiles (plasma density, velocity, electron and ion temperatures), which are used for the impurity transport analysis with the IMPGYRO code, are calculated from the SOL/divertor simulation code (B2-Eirene code [9]). The model geometry and numerical mesh used in the B2-Eirine calculation are shown in Fig. 1(a), which are generated from a JT-60U MHD equilibrium. The bulk deuterium ion (D^+) density at the core interface boundary (CIB) is set to be $n_D = 3.6\times10^{19}\,\mathrm{m}^{-3}$. The total input power at the CIB is taken to be 2.5MW and equally delivered to the electrons and ions.

The results for the electron density and electron temperature in the divertor region are shown in Fig. 2(a) and (b), respectively. As seen from Fig. 2(b), the electron temperature in front of the divertor plates becomes very low and divertor plasma is considered to be in a typical power detachment state.

2.3 Initial and Boundary condition for the IMPGYRO simulation

In this study, a relatively simple assumption has been used for the primary impurity generation, i.e., the first generation of the impurities: 1 test particle per 100 time-step ($\Delta t = 1\times10^{-9}$ sec) is uniformly launched from the inner and the outer divertor plate as a neutral tungsten with monotonic energy of 10eV and cosine angular distribution.

In the previous study[4], the numerical mesh in Fig. 1(a) is used not only for the background plasma calculation, but also for the impurity transport analysis by the IMPGYRO code. The simple boundary condition, i.e., the absorbing boundary condition was imposed on the following boundaries in Fig. 1(a): 1) the wall-side boundary (WSB), 2) the core-interface boundary (CIB), and 3) the dome-side boundary in the private region (DSB). Test particles reaching these boundaries are simply removed from the calculation domain without any self-sputtering and/or reflection.

To impose more realistic boundary condition, the calculation domain for the IMPGYRO code has been

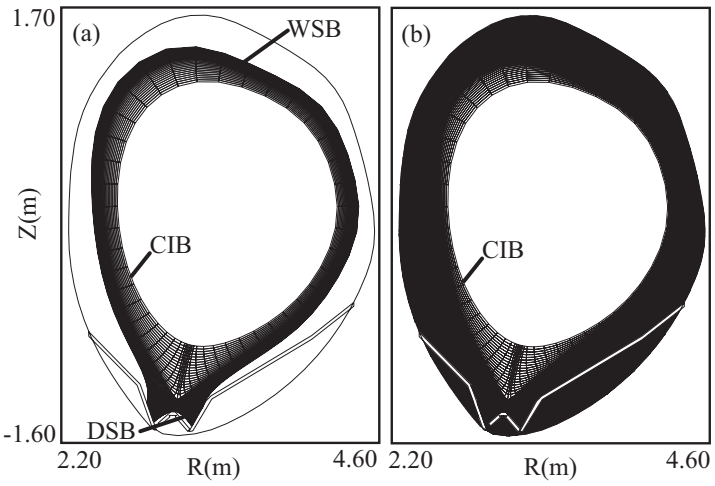

Fig. 1 Numerical meshes: (a) for background plasma calculations and (b) extended meshes used for the IMPGYRO code

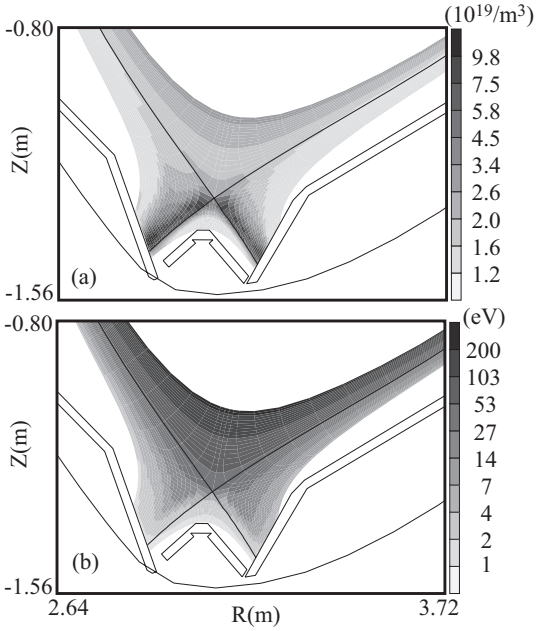

Fig. 2 Back ground plasma profiles: (a) electron density and (b) electron temperature

extended in this study as shown in Fig. 1(b). Test particles reaching the WSB and the DSB described above are not removed, but their trajectories are followed until they reach the boundaries of the real structures, i.e., the first wall, baffle plate and dome structures. The spatial variations of the magnetic field for the extended domain in Fig. 1(b) have been taken into account in the calculation of the particle trajectories, while the simple exponential decay of the background plasma profiles has been assumed with the decay length 0.1m in the direction perpendicular to the magnetic flux surface.

3. Numerical results and Discussion

Numerical calculations have been done for the following two cases: 1) Case A with extended numerical meshes in Fig. 1(b), i.e., with more realistic boundary condition discussed above, 2) Case B with numerical meshes in Fig. 1(a).

Figure 3 shows the time evolutions of the total number of test tungsten particles (neutral and ions) N_T in the system for the Case A and Case B. Due to the effect of the re-emission mainly from the dome surface, the total number for Case A in the steady state becomes larger than for Case B. More quantitative discussion of this difference will be given later. Figure 4 shows the 2D density profiles of tungsten in the core edge region near the X-point and the divertor region in the quasi–steady state in Fig. 3. The profiles in Fig. 4 suggests that tungsten particles mainly cross the separatrix near the X-point and penetrate into the core under the detachment plasma condition. It is confirmed that the particles flow inward by checking the particle trajectories. In the attached case, however, impurities penetrating into the core are few. In this case, impurities are ionized as soon as they are released from the plates, and they receive the friction force toward the plates.

To understand the difference of N_T in Fig. 3 for Case A and Case B in the steady state, the following simple and global model of particle balance is useful:

$$\frac{dN_T}{dt} = S - \frac{N_T}{\tau_p} + \frac{N_T}{\tau_p}\sum_i \alpha_i \gamma_i \,, \qquad (1)$$

where S is the total source rate of the primary impurity, the second term N_T / τ_p expresses the total loss rate, i.e., the total number of the impurity particles reaching the boundary per unit time. The global confinement time without the effect of the recycling process (reflection and/or self-sputtering) is denoted by τ_p. The τ_p is so called the "intrinsic" confinement time, because it does not include the effect of the particle recycling. The effect of particle recycling is taken into account in the last term in Eq. (1). The symbol α_i denotes the fraction of the particles reaching the i-th boundary, while γ_i denotes the particle re-emission yield of the i-th boundary. For Case A, the calculation boundary has been classified into the following sub-boundaries, 1) inner divertor plate, 2) outer divertor plate, 3) inner and outer baffle plates, 4) first wall and 5) dome structure in the private region as shown in Fig. 1(b). On the other hand, 1) WSB, 2) inner divertor plate, 3) outer divertor plate, 4) CIB, and 5) DSB in Fig. 1(a) are used for Case B. For example, if i = inner divertor plate, then $(N_T / \tau_p)\alpha_i$ expresses the total number of impurity particles reaching the inner divertor plate per unit time, and $(N_T / \tau_p)\alpha_i \gamma_i$ describes the total number of particles recycling from the inner divertor

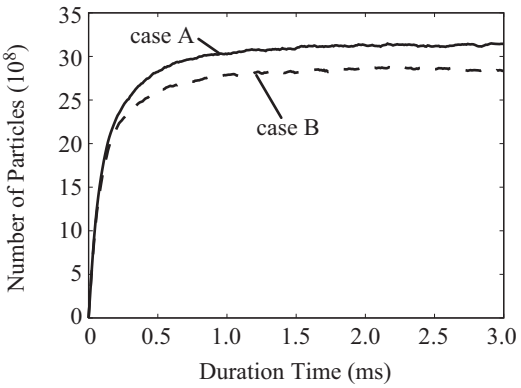

Fig. 3 Time evolutions of the total number of test impurity particles are compared: Case A with the extended meshes and Case B with the previous meshes

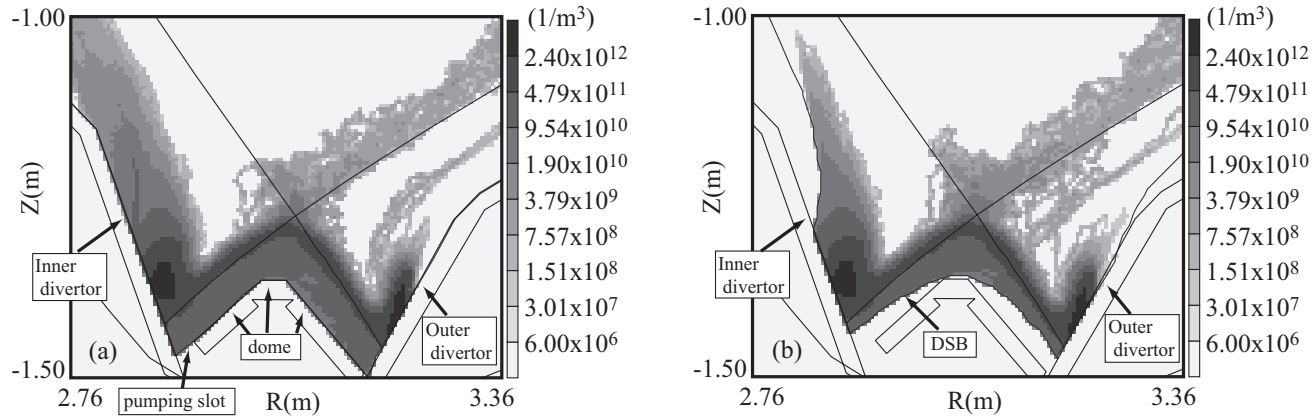

Fig. 4 Two-dimensional spatial profiles of impurity density (the sum of the each charge state): (a) Case A with the extended meshes and (b) Case B with the previous meshes

plate per unit time.

From Eq. (1), the total number of particles N_T in the steady state can be estimated by

$$N_T = S\tau_p^*, \quad \tau_p^* = \tau_p / (1 - \sum_i \alpha_i \gamma_i) . \qquad (2)$$

where τ_p^* is the effective confinement time including the re-emission process. The source rate S for Case A and Case B are the same, because the injection rate of the primary impurity is the same for both cases. Therefore, the ratio of the total number of test particles in the steady state becomes the ratio of the effective confinement time for the Case A and Case B, i.e.,

$$N_T^A / N_T^B = \tau_{p,A}^* / \tau_{p,B}^* . \qquad (3)$$

To calculate this ratio, it is necessary to estimate the intrinsic confinement time τ_p and the parameters α_i, γ_i in Eq. (2). The former, i.e., τ_p is obtained from the following manner. After the system reaches the steady state, the injection of the primary impurity is stopped and all the calculation boundaries are set as absorbing boundary. Then, the number of the impurity in the system starts decreasing. From this time-decay of N_T, τ_p for Case A and Case B are estimated to be $\tau_{p,A} \approx 0.136$ms and $\tau_{p,B} \approx 0.123$ms, respectively. The reason of the increment for Case A is that the survival time of impurity particles becomes longer, due to the larger system size. The fraction α_i of the particles reaching the *i*-th boundary, and the re-emission yield γ_i from the *i*-th boundary are summarized in Table 1(a) for Case A and 1(b) for Case B, respectively. A lot of impurities are pushed back to the divertor plates by the friction force. Therefore, the impurities crossing the core interface boundary are almost zero, but they are not completely zero at least under the present calculation condition. From these values in Table 1 and τ_p, we finally obtain $\tau_{p,A}^* \approx 0.42$ms, $\tau_{p,B}^* \approx 0.34$ms and the ratio as $N_T^A / N_T^B \approx 1.24$ from Eqs. (2) and (3), which reasonably agrees with the value $N_T^A / N_T^B \approx 1.1$ directly calculated from the simulation result in Fig. 3.

Table 1 Parameters α and γ for each boundary (a) Case A with the extended meshes and (b) Case B with the previous meshes

(a) Case A

	α (%)	γ (%)
Inner divertor	32.8	68.2
Outer divertor	53.2	72.9
CIB	~0	---
wall	~0	80.0
dome	12.6	48.6
buffle	0.5	63.9
pumping slot	0.9	---

(b) Case B

	α (%)	γ (%)
Inner divertor	35.3	68.2
Outer divertor	55.4	71.5
CIB	~0	---
WSB	0.2	---
DSB	9.0	---

As mentioned above, all the particles reaching the WSB and the DSB are removed, and the re-emission yield γ is set to be zero for these boundaries for Case B. On the other hand, for Case A, γ becomes 0.80 and 0.486, respectively, for the wall and the dome structure. The fraction α_i of the particles reaching these boundaries, however, relatively small in comparison with those reaching the inner and outer divertor plates as seen from Table 1(a). Therefore, the recycling effect of these boundaries on the global confinement of impurities in the system, i.e. the effect on the ratio N_T^A / N_T^B is relatively small.

4. Summary and future plan

To improve the boundary condition used in the previous analysis by the coupled IMPGYRO-EDDY code[4] and to evaluate more correctly the effect of the re-emission process on the dome, baffle and wall surfaces, the numerical mesh has been extended to the low density and low temperature regions in front of these surfaces. The transport analysis has been done for the typical detached condition in the model geometry of tokamak. The numerical results have been checked by using the simple analytic model of the global particle balance. The ratio of global-confinement time in the numerical simulation reasonably agrees with that obtained from the simple analytic model.

Above test calculation shows the IMPGYRO code is useful tool to analyze the high-Z transport process in the experiments. The code, however, is still under the development and it is necessary to couple to the background plasma code for more self-consistent simulations for the final goal.

Acknowledgement

This study is partially supported by a Grant-in-Aid for Scientific Research of the Japan Society for the Promotion of Science.

[1] I. Hyodo, *et al*., J. Nucl. Mater. **313-316** (2003) 1183.
[2] A. Fukano, *et al*., J. Nucl. Mater. **363-365** (2007) 211.
[3] K. Hoshino *et al*., Contrib. Plasma Phys. **48** (2008) 280.
[4] M.Toma *et al.*, "*Coupled IMPGYRO-EDDY simulation of tungsten impurity transport in a realistic tokamak geometry* ", *in Proc. of 18th International Conference on Plasma Surface Interactions in Controlled Fusion Devices*, Toledo, Spain, May 2008.
[5] T.Takizuka, *et al.*, J.Comp.Phys. **25** (1977) 205.
[6] J.Neuhauser, *et al.*, Nucl.Fusion **18** (1984) 39.
[7] K.Asmussen, *et al.*, Nucl.Fusion **38** (1998) 967.
[8] K. Ohya, Physica Scripta **T124** (2006) 70.
[9] R. Schneider, *et al*., Contrib. Plasma Phys. **46** (2006) 3-191.